Seventh International Conference on Computational Fluid Dynamics (ICCFD7), Big Island, Hawaii, July 9-13, 2012

ICCFD7-3105

Progress and Challenges in Liquid Rocket Combustion Stability Modeling

V. Sankaran*, M. Harvazinski**, W. Anderson** and D. Talley*
Corresponding author: venkateswaran.sankaran@edwards.af.mil

* Air Force Research Laboratory, Edwards AFB, CA, USA
** Purdue University, West Lafayette, IN, USA

Abstract: Progress and challenges in combustion stability modeling in rocket engines are considered using a representative longitudinal mode combustor developed at Purdue University. The CVRC or Continuously Variable Resonance Chamber has a translating oxidizer post that can be used to tune the resonant modes in the chamber with the combustion response leading to self-excited high-amplitude pressure oscillations. The three-dimensional hybrid RANS-LES model is shown to be capable of accurately predicting the self-excited instabilities. The frequencies of the dominant first longitudinal mode as well as the higher harmonics are well-predicted and their relative amplitudes are also reasonably well-captured. Post-processing the data to obtain the spatial distribution of the Rayleigh index shows the existence of large regions of positive coupling between the heat release and the pressure oscillations. Differences in the Rayleigh index distribution between the fuel-rich and fuel-lean cases appears to correlate well with the observation that the fuel-rich case is more unstable than the fuel-lean case.

Keywords: Combustion Instability, Liquid Rocket Engines, Reacting Flow.

1 Introduction

Combustion stability presents a major challenge to the design and development of liquid rocket engines. Instabilities are usually the result of a coupling between the combustion dynamics and the acoustics in the combustion chamber. They can cause increased vibration, spikes in heat transfer, flashback, flame blow-off, and uncontrolled impulse. In some instances, these phenomena can be so extreme that catastrophic failure of the engine can occur within a period of less than one second. Research on combustion instability in liquid rocket devices was very active in the 1950's and 1960's but has been more erratic since. In most engine development programs, instabilities were typically eliminated or mitigated using a test-driven strategy during the design phase. A notable instance of this approach was the development of the F-1 liquid rocket engine for the Apollo mission. From 1962 to 1965, the F-1 underwent over 2000 full-scale tests resulting in a four-year delay [1]. Because of the challenges of the modeling of the fundamental physical phenomena in liquid rocket engines, most other major engine developments have taken a similar path [2]. Given present-day resource limits, it is crucial to develop a model-driven strategy to mitigate combustion instabilities in liquid rocket engine design. To date no comprehensive model exists which can accurately predict the level of instability that occurs for a particular engine and operating condition [3, 4, 5]. The objective of this article is to document the current status of high-fidelity physics-based models and to describe the inherent challenges faced by these models.

The coupling between heat release and pressure is the fundamental source of most instabilities. The relationship was first recognized by Lord Rayleigh in 1878 [6], later described mathematically by Putnam

and Dennis in 1953, and further refined by Zinn in 1992 [7],

$$\mathcal{R} = \frac{1}{t_f - t_0} \int_{t_0}^{t_f} \int_{\Omega} p'(x,t) q'(x,t) d\mathcal{V} dt \tag{1}$$

The Rayleigh criterion states that for positive values of $\mathcal{R}$ the heat release and pressure are in-phase and the acoustic modes are driven or amplified. For negative values, the heat release and pressure are out-of-phase and the acoustic modes are dampened. While Eqn. 1 is simple the underlying physics are complex and difficult to predict. The amplitude of the instability is a function of the engine geometry, operating conditions and fuel type. Moreover, the fraction of the combustion energy that is coupled with the acoustic modes is controlled by a fine balance between competing physical processes such as injection, atomization, vaporization, mixing, and combustion, and their individual and combined responses to the driving acoustic fluctuations.

There are several challenges associated with modeling combustion instability in liquid rocket engines. For one, the pressure in a rocket engine can be extremely high, 6-20 MPa, with the cryogenic propellants operating at super-critical pressures, but sub-critical temperatures. Such conditions require the use of appropriate equations of state and the ability to handle the associated multi-phase phenomena involving large density ratios and a wide range of velocity scales. Moreover, detailed flow diagnostics are extremely limited under such harsh operating conditions, which in turn means that it is difficult to obtain good validation data to anchor the predictions. A further issue is the importance of turbulence and combustion phenomena. Combustion instability involves inherently unsteady fluid dynamics requiring large eddy simulations (LES) or hybrid RANS/LES computations. Moreover, the reacting flow requires the modeling of detailed chemical kinetics mechanisms which can involve large numbers of chemical species and reactions (particularly for hydrocarbon fuels). Finally, since the combustion typically occurs at sub-grid scales, appropriate turbulent combustion closure models may be needed for capturing the relationship between the heat release and the acoustic modes.

Besides the complexity of the physical models, the geometric configuration of liquid rocket combustors introduces further modeling issues. Acoustic modes in the combustor are strongly influenced by appropriate boundary condition specification at the injector face. However, the difficulty of obtaining detailed diagnostic information at this location means that it is difficult to characterize these boundary conditions very well. It is therefore necessary for rocket chamber computations to include the propellant flow field in the injector posts all the way up to the injector manifolds, which may be more acoustically isolated from the chamber. Typical rocket combustors contain hundreds of injectors and the inclusion of the injector post flowfields adds significantly to the complexity and grid requirements for these simulations. A related issue is the massive amounts of data that are generated by these simulations and the concomitant challenge of mining these data for pertinent physical interactions of significance to driving the combustion instability phenomena. The so-called "big-data" problem is therefore another major pacing element in the fundamental understanding of combustion instabilities.

To address these challenges, the Air Force Research Laboratory has embarked on a combined modeling and experimental effort called the Advanced Liquid Rocket Engine Stability Stability Technology Program (ALREST). This is a nationally coordinated data-centric multi-fidelity approach for modeling combustion stability in rocket engines. It consists of both modeling and experimental components and is data-centric in the sense that all modeling activities are targeted towards experimental datasets of different stable and unstable combustor configurations. The analysis paradigm is based on a multi-fidelity suite of tools ranging from high-fidelity LES codes to lower-fidelity acoustics and Euler equation codes. As shown in Figure 1, the overall vision encompasses not only the validation of the high-fidelity predictions with high-resolution experimental data, but also the extraction of response functions that can be used to improve the predictions of the lower-fidelity engineering models. ALREST is highly coordinated through workshops and meetings with other efforts funded by AFOSR and NASA.

The current article summarizes the state-of-the-art of high-fidelity physics-based modeling of combustion stability in liquid rocket engines by considering both experimental and computational efforts related to a longitudinal mode combustor configuration being tested at Purdue University. In the following section, we present the details of the experimental configuration and computational models used in the Purdue GEMS code. In the next section, we present the computational predictions and comparisons to the experimental

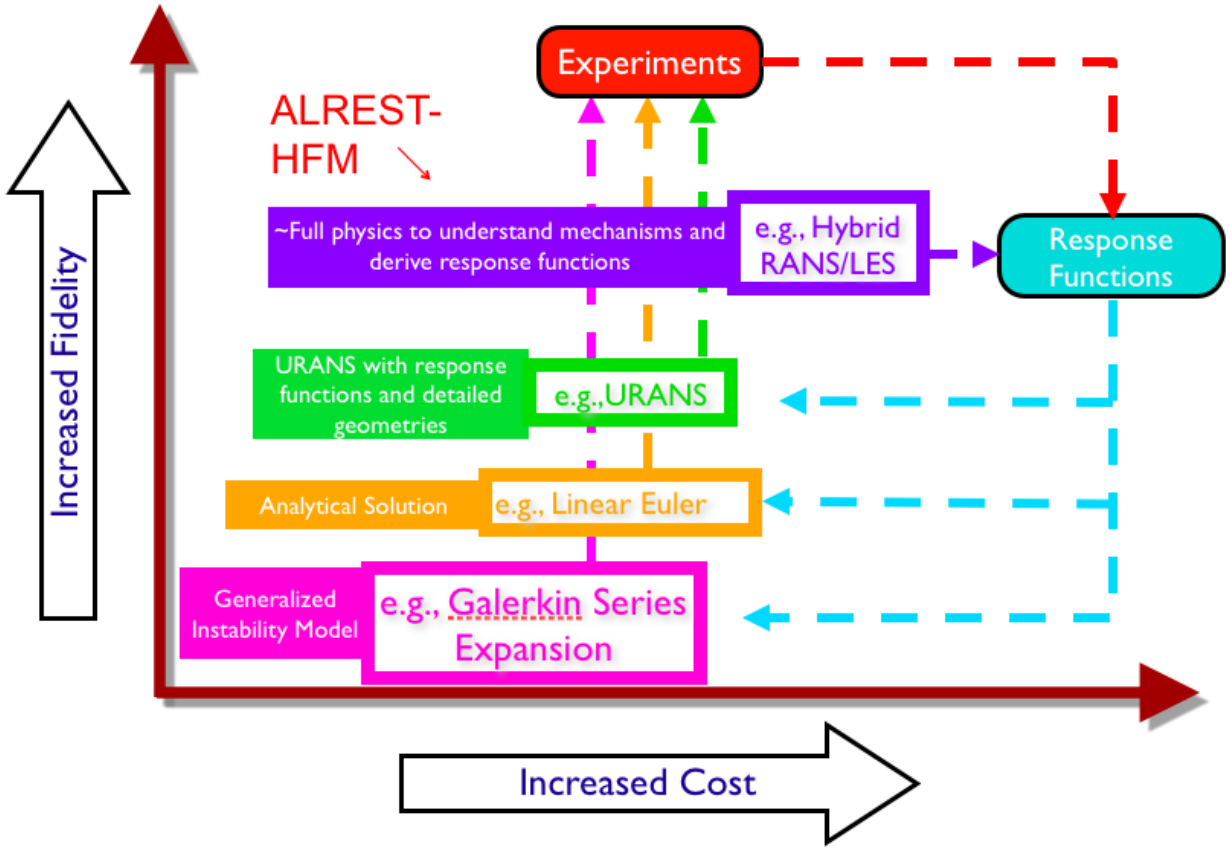

Figure 1: Multi-fidelity model cascade for liquid rocket engine combustion stability predictions.

results. We demonstrate how this combined experimental-computational approach can be instrumental in improving our understanding of combustion dynamics and their influence on combustion instability. We conclude by providing a summary of the status of combustion stability modeling and outlining future research and development directions.

2 Continuously Variable Resonance Chamber Experiment

In this section, we describe a representative combustion stability experiment and companion computational efforts, both carried out at Purdue University. The experiments concern a model rocket engine known as the Continuously Variable Resonance Chamber or CVRC shown in Figure 2, that is designed to excite and sustain longitudinal mode instabilities in a single-element rocket engine. The CVRC configuration is capable of varying the length of the oxidizer post by moving the location of the choked inlet in the oxidizer tube, which in turn enables the tuning of the instability modes in the combustor. A catalyst bed decomposes liquid hydrogen peroxide into hot steam and oxygen for use as the oxidizer. The fuel is injected through a coaxial slot located in the injector element just upstream of the combustion chamber. Several fuel types have been used but the majority of the work as been with gaseous methane. The design of the experiment was done in recognition of computational fluid dynamics (CFD) simulation needs, particularly related to the specification of well-defined boundary conditions. The combustor itself is 15 in (38.1 cm) long and is cylindrical with a radius of 0.885 in (2.250 cm). A choked converging diverging nozzle is attached to the downstream end of the combustor. The rig is outfitted with a number of high-speed pressure transducers which collect data at a rate of 100 kHz. A complete description of the experiment is available in Yu [8].

The oxidizer post length is varied from 3.5 in to 7.5 in, (8.89 cm to 19.05 cm). By varying the post length, the acoustic resonance of the chamber changes and allows the combustor to operate at both stable and

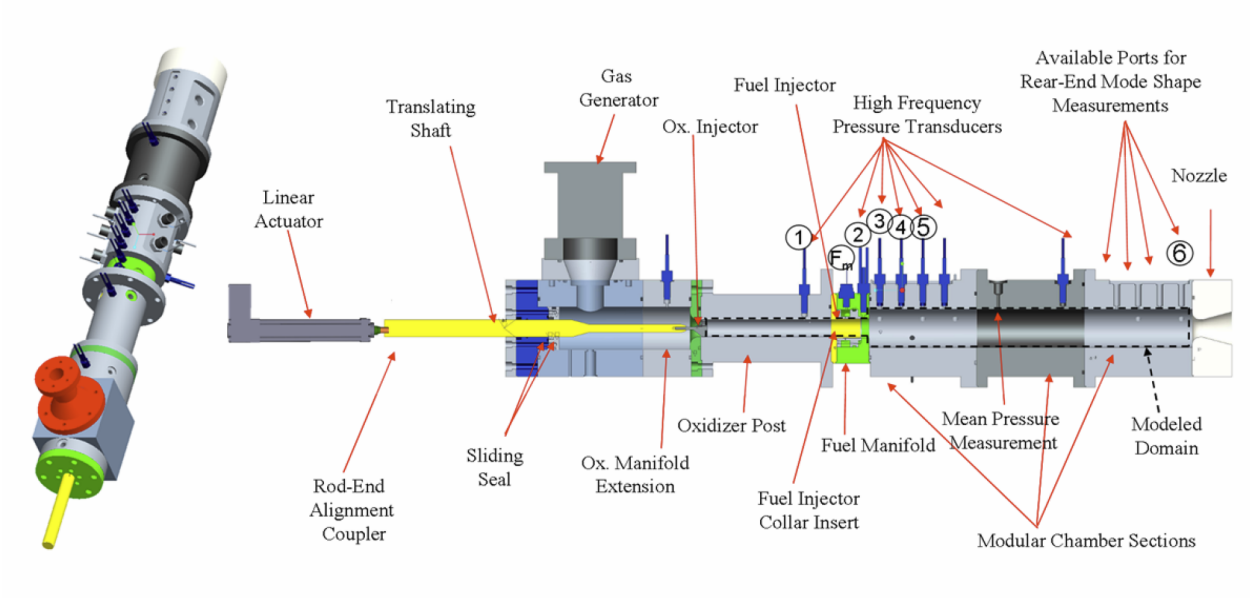

Figure 2: Experimental schematic for the CVRC rig [8].

unstable conditions. The transition from stable to unstable (or unstable to stable) is observed to occur both when the oxidizer post length is increasing and when it is decreasing. Forward and backward translation results in similar behavior with a slight hysteresis in the transition length depending on the direction of movement. The rig can also operate at fixed lengths and the levels of instability are comparable to that of the translating tests. Once the transition from stable to unstable combustion takes place, a limit cycle is reached where the pressure in the combustor is oscillating but is neither growing nor decaying. Typical peak-to-peak pressure amplitudes during the limit cycle are 120 psi (827 kPa), which can be as high as 50% of the mean chamber pressure. Representative data for the experiment are shown in Figure 3. Additional experimental data may be found in Refs. [8, 9, 10]. The condition shown is for the 5.5 in oxidizer post length. The Power Spectral Densities (PSD) show the well-ordered harmonic nature of the instability with well-defined peaks occurring at integer multiples of the first mode. The pressure at the 3.5 in location shows a lower level of instability due to its proximity to a pressure node located near 3.75 in.

Companion simulations are conducted using a CFD code developed at Purdue University called the General Equation and Mesh Solver or GEMS [11, 12]. GEMS is a finite volume code that is capable of solving the coupled Navier-Stokes equations along with an arbitrary number of species equations for both reacting and non-reacting configurations. The code uses an implicit formulation with dual-time stepping to reduce approximate factorization errors and to efficiently handle the high-aspect ratio cells in the boundary layer. The code is second order accurate in both time and space. Turbulence is modeled using a hybrid LES/RANS approach with a two-equation k-ω turbulence model used for the near wall region [13, 14, 15, 16]. Combustion is treated with a single-step global reaction and laminar closure is typically used for the evaluation of the combustion source term. Additional details of the code are available elsewhere [17, 18, 19, 20, 21, 22].

The computational configuration is shown in Figure 4. The oxidizer manifold and combustor are acoustically isolated from the combustion chamber which allows boundary conditions to be imposed in these regions without knowledge of the dynamic response of the boundary to the pressure oscillations in the combustion chamber. In the case of oxidizer post, the simulation domain includes the choked slots that are located in-between the oxidizer manifold and the oxidizer post and the boundary conditions are held fixed in the manifold that is upstream of the slots. A number axisymmetric and three-dimensional simulations have been carried out. The representative 3D simulations shown here use approximately 5 million grid points. The grid at the wall is refined to a y^+ of one to resolve the boundary layer in the RANS region. Wall boundaries are considered adiabatic and the no-slip condition is enforced. Both the oxidizer and fuel inlet boundary conditions are defined using a specified mass flow, total temperature, and appropriate species fractions. The

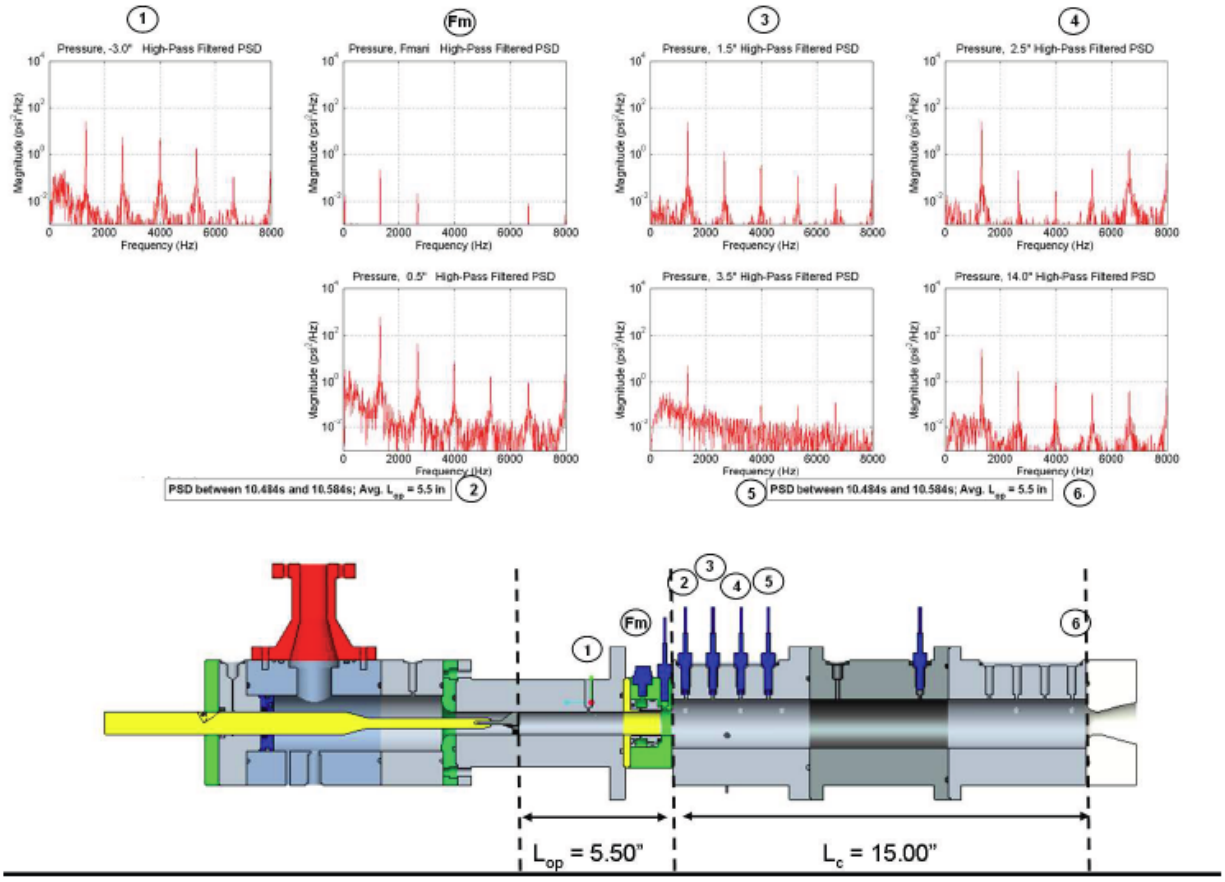

Figure 3: Experimental results for the 5.5 *in* oxidizer post length [8].

nozzle outlet boundary condition is defined using a back-pressure of 101.325 kPa. For comparison purposes, representative axisymmetric results using similar mesh resolution (55,000 grid points) as the 3D case and much finer mesh resolution (200,000 points) are also given.

Simulations start from quiescent conditions at a uniform pressure of 140 kPa. At the beginning of the simulation oxidizer and fuel begin to flow from the inlets and after about 2 ms ignition takes place. Combustion occurs for the remainder of the simulation and for the unstable conditions studied, the results are observed to be spontaneously unstable. In the results shown here, two equivalence ratios are simulated: a fuel lean case with an equivalence ratio of 0.8 and a fuel rich case with an equivalence ratio of 1.4. The two equivalence ratios are obtained by varying the fuel mass flow, while all other operating conditions remain identical. Additional computational results are available elsewhere [23, 24, 25]. In the following section, various representative computational solutions are shown and compared with available experimental data.

3 Computational Results

We first present representative three-dimensional results for the fuel-rich case. As mentioned earlier, the computational results predict self-excited instabilities. The oscillations grow until they reach a limit cycle at which amplitude the energy added is presumably balanced by the energy lost due to heat transfer, convection and viscous dissipation. Figure 5 shows iso-contours of the heat release near the head-end of the combustion chamber for a sequence of time-steps within a single cycle of the dominant acoustic mode. It is apparent that the flame zone is highly dynamic with the heat release occurring cyclically during the period. In particular, the flame appears to undergo sequential extinction and re-ignition during the cycle. Superimposing the pressure contour (not shown) reveals that the heat release appears to be approximately synchronized with

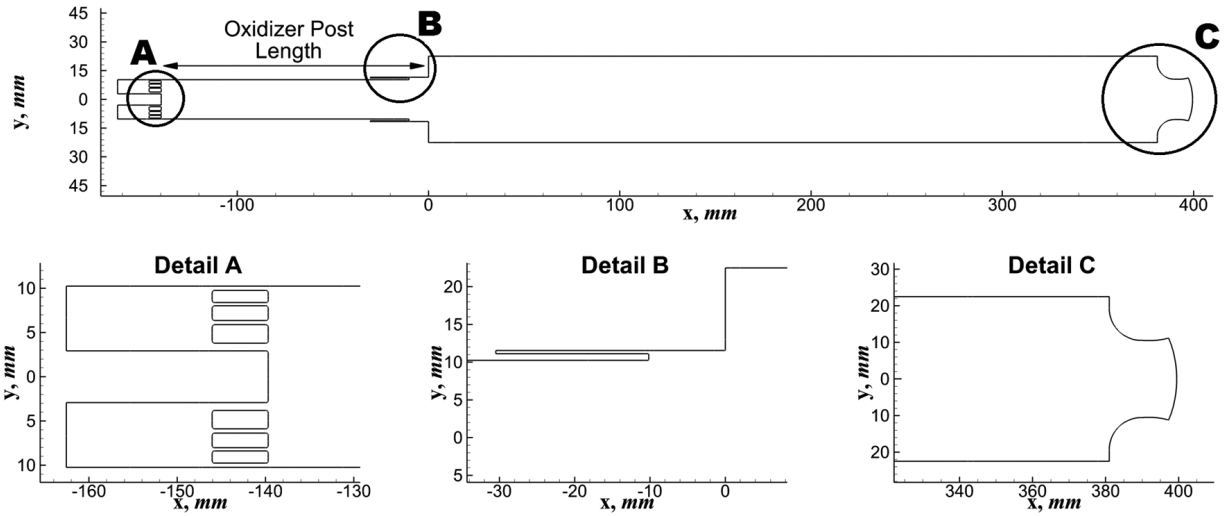

Figure 4: Computational domain for CVRC experiment. Detail A shows the slotted oxidizer inlet, detail B shows the fuel injector and backstep and detail C shows the converging diverging nozzle at the downstream end [12].

the pressure wave. Higher levels of heat release occur when the pressure is at a maximum and lower levels occur when the pressure is at a minimum. There is also substantial spatial variation in the heat release contours which further complicates the picture. Recalling the Rayleigh criterion that was discussed earlier, the trends appear consistent with the occurrence of combustion instabilities.

The results shown here are for the three-dimensional case, although qualitatively similar results are obtained for the axisymmetric equivalent-mesh and fine-mesh cases as well. It is instructive to look at the vorticity field for the three computations, as shown in Figure 6. The figure shows the flowfield in the oxidizer post and the head-end of the combustion chamber. It is clear that there is significant vorticity generation just downstream of choked slots in the upstream section of the oxidizer post. The 3D results show that the vorticity is damped as the flow proceeds down the length of the post. In contrast, the axisymmetric results show the vortices persisting much longer and, particularly in the fine-mesh case, the vorticity appears very strong even as the flow enters the head-end of the combustion chamber. The lack of adequate vorticity damping in the axisymmetric case is related to the absence of the vortex stretching term that is an important aspect of the turbulent energy cascade. Importantly, the persistence of the vorticity from the oxidizer post into the combustion chamber means that the axisymmetric simulations will likely be less accurate than the 3D simulations.

Figure 7 shows corresponding wall-pressure data (obtained at a single wall location) as a function of time for the three computational cases as well as comparisons with experimentally measured pressures. In all cases, the perturbation pressure, i.e., the instantaneous pressure minus the mean pressure, is plotted versus time. It is noteworthy that the 3D wall pressures agree remarkably well with the experimental measurements both in terms of the wave shape and the amplitude. In contrast, the axisymmetric simulations show considerably more noise in the wave shapes and noticeably lower amplitudes in the oscillations. The noise in the axisymmetric results is probably related to the excessive vorticity in the flow at the head-end of the combustor. The lower amplitudes are more difficult to explain, but it appears that the stronger three-dimensional mixing may be leading to more concentrated heat release contours and correspondingly higher values of the Rayleigh index.

Power spectral densities related to the three cases and the corresponding experimental results are shown in Figure 8. Again, the 3D results agree very well with the experimental results while the axisymmetric results show poorer agreement. In the 3D case, the mode frequencies are accurately predicted and the amplitudes are also reasonably captured. Moreover, the relative amplitudes of the dominant first longitudinal mode and the higher harmonics are also well-predicted. In contrast, the axisymmetric results only show the dominant unstable mode. The excitation of the high harmonics appears more muted and assumes more of a broad-band

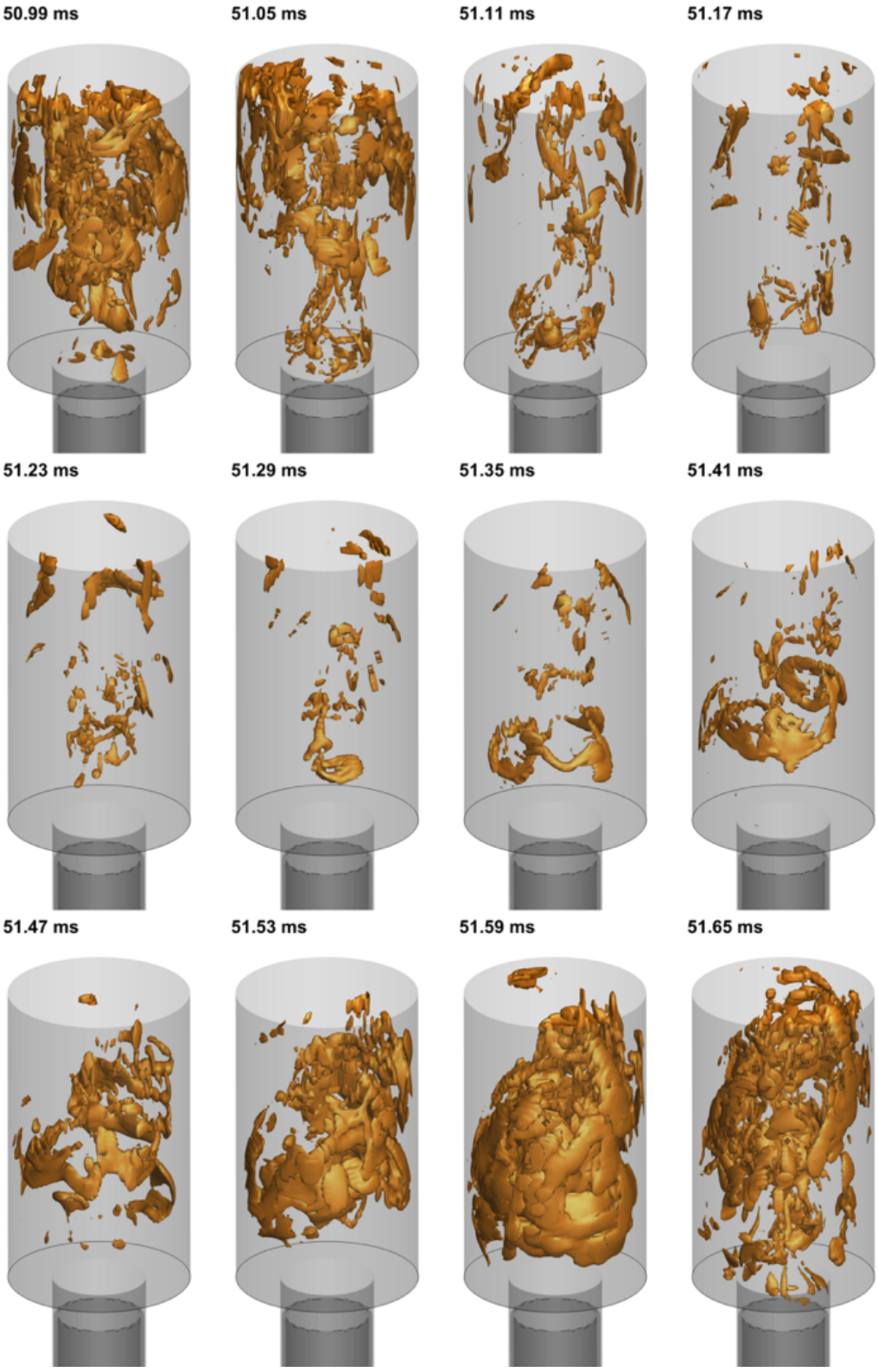

Figure 5: Representative unsteady combustion flow field showing iso-contours of the heat release [12].

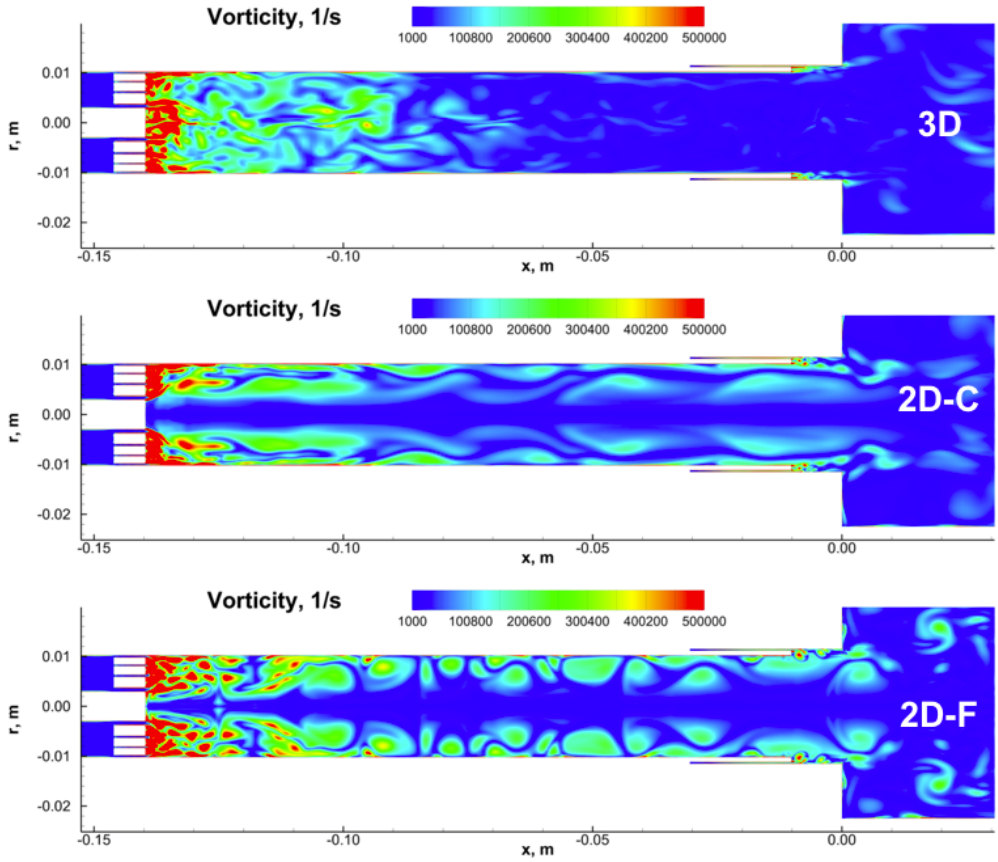

Figure 6: Vorticity field in oxidizer post and head-end of combustion chamber using full-3D configuration as well as axisymmetric configuration with coarse and fine grids [12].

character. Moreover, the amplitude of even the most unstable mode is grossly under-predicted. Indeed, these observations appear consistent with our earlier observations related to the persistence of vorticity and the lower levels of mixing in the axisymmetric cases.

Figure 9 shows the mode-shapes obtained from the computed wall pressure data of the 3D case. The first and second modes of the pressure and velocity variables are given. They are obtained by filtering the computed data at the frequencies of the first two acoustic modes. It should be pointed out that the mode shapes are given for the entire configuration, i.e., both in the post and the combustion chamber, and the head-end of the combustor is located at $x = 0\ m$. From the mode shapes, it is clear that the first two acoustic modes in the combustion chamber resemble the classic modes in an open tube. The presence of the oxidizer post, however, introduces some variation in the mode shapes—for instance, the pressure and velocity nodes are not very tight and the head-end location does not exactly correspond to a pressure anti-node and a velocity node. In fact, we recall that the CVRC configuration is dependent on tuning the oxidizer post length to drive the instabilities in the chamber. The mode shapes therefore provides some insight as to how the combustor modes couple with those in the post. Specifically, we note that changing the length of the oxidizer post results in a variation in the acoustic mode frequencies, which in turn determine the overall stability response of the configuration.

Similar results for the fuel-lean case are shown in Figure 10. Here, we show the power spectral densities for the 3D simulations of the fuel-rich and fuel-lean case. It is observed that the first longitudinal mode is the most unstable frequency in both cases. However, the fuel-rich case displays higher instability amplitudes indicating that it is somewhat more unstable than the fuel-lean case. Experimental measurements (not shown here) also show similar trends. Figure 11 shows the computed Rayleigh indices for the two cases. The fuel-lean case is observed to have regions of positive Rayleigh index indicating growth as well as regions of

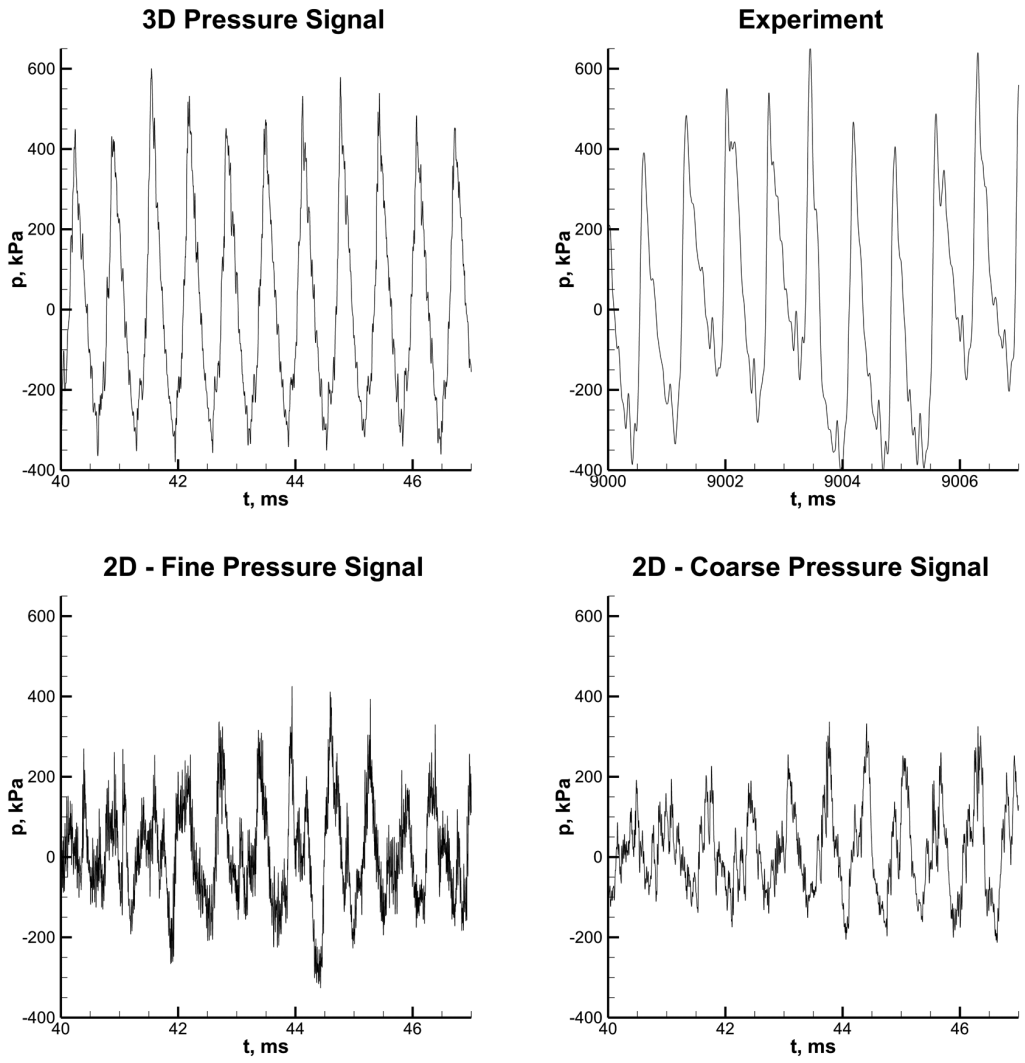

Figure 7: Time-dependent wall pressure oscillations over a few cycles for 3D and coarse- and fine-axisymmetric configurations as well as experimental data [12].

negative Rayleigh index indicating damping. On the other hand, the fuel-rich case appears to have only a strong growth region, while the negative damping region appears to be largely absent. While these are only two data points, the results seem to correlate well with the larger instability observed in the fuel-rich case.

4 Conclusions

The article provides a summary of the status of combustion stability modeling in rocket engines. Combustion instabilities are the result of the coupling between the combustion dynamics and the acoustic modes in the combustion chamber. In liquid rocket engines, this coupling is governed by complex physical phenomena such as fuel and oxidizer injection, atomization, vaporization, mixing and combustion and first principles modeling is very challenging. Large eddy simulations or hybrid RANS/LES modeling with appropriate chemical kinetics and turbulent combustion closures may be needed to capture the detailed flame dynamics and the acoustic response. It is further necessary to enforce boundary conditions in acoustically isolated regions of the flow, which means that the computational domain may need to include the fuel and oxidizer manifolds in addition to the combustion chamber itself. Moreover, the ability to handle large amounts of

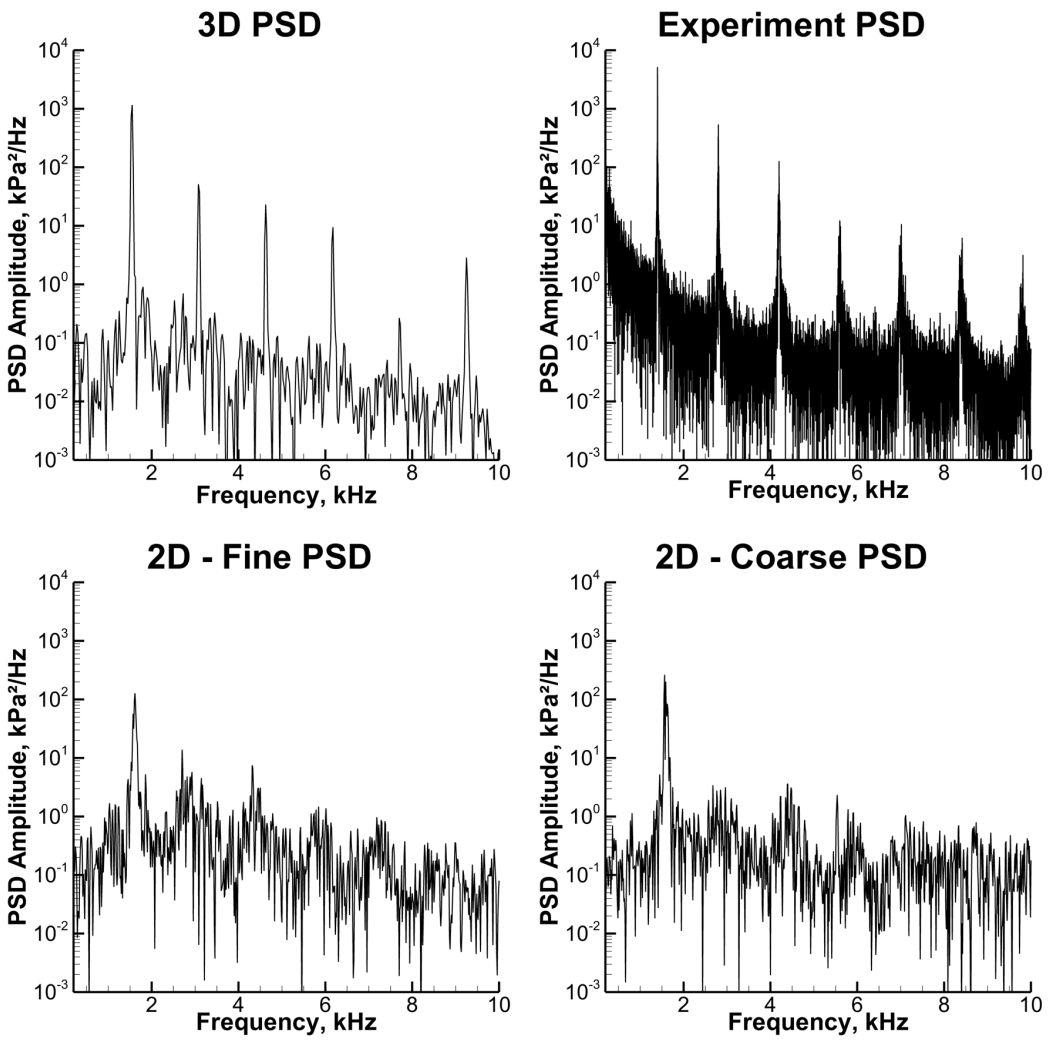

Figure 8: Power spectral density for wall pressure oscillations for 3D and coarse- and fine-axisymmetric configurations as well as experimental data [12].

data and to extract the essential underlying features are also an important aspect sof combustion stability modeling.

To address these challenges, the Air Force Research Lab has instituted the ALREST (Advanced Liquid Rocket Engine Stability Technology) program. ALREST involves a data-centric and multi-fidelity model development approach that is nationally coordinated. The analysis paradigm employs models of variable fidelity ranging from LES to engineering stability models. The analyses are targeted at datasets of stable and unstable configurations, which are used to validate the high-fidelity simulations as well as to extract response functions which can be utilized in lower-order models. The present article considers one representative experimental dataset, namely Purdue University's CVRC (Continuously Variable Resonance Chamber), which is a self-excited longitudinal mode experiment. Computational predictions using Purdue University's GEMS code are presented and compared with the experimental measurements.

The overall conclusions of the CVRC configuration are that three-dimensional simulations are necessary to properly capture the combustion dynamics. The 3D results provide an accurate prediction of the frequencies of the self-excited instability modes and a reasonable prediction of their relative amplitudes. In comparison, the axisymmetric results correctly predict only the dominant first-mode, while the higher harmonics are not captured very sharply. Moreover, the amplitude of the pressure oscillations are severely under-predicted

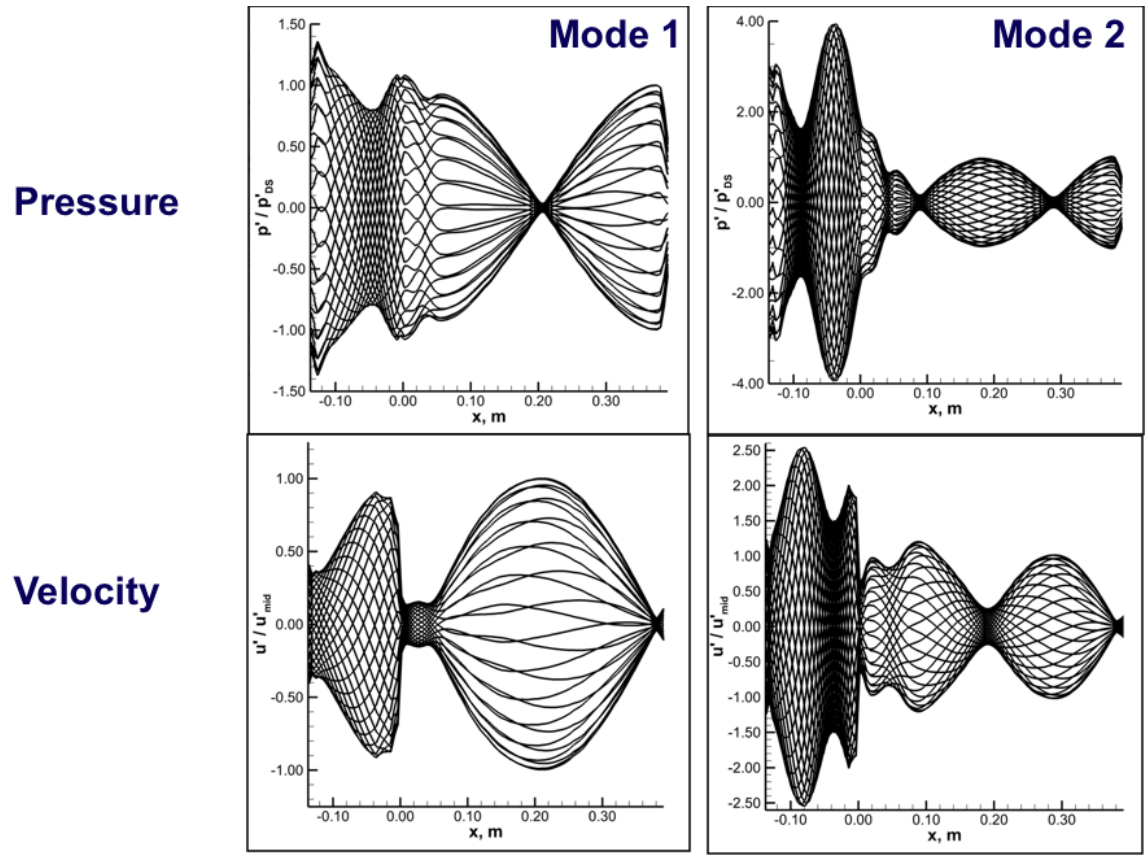

Figure 9: Filtered pressure and velocity distributions for first and second acoustic modes in the CVRC configuration [12].

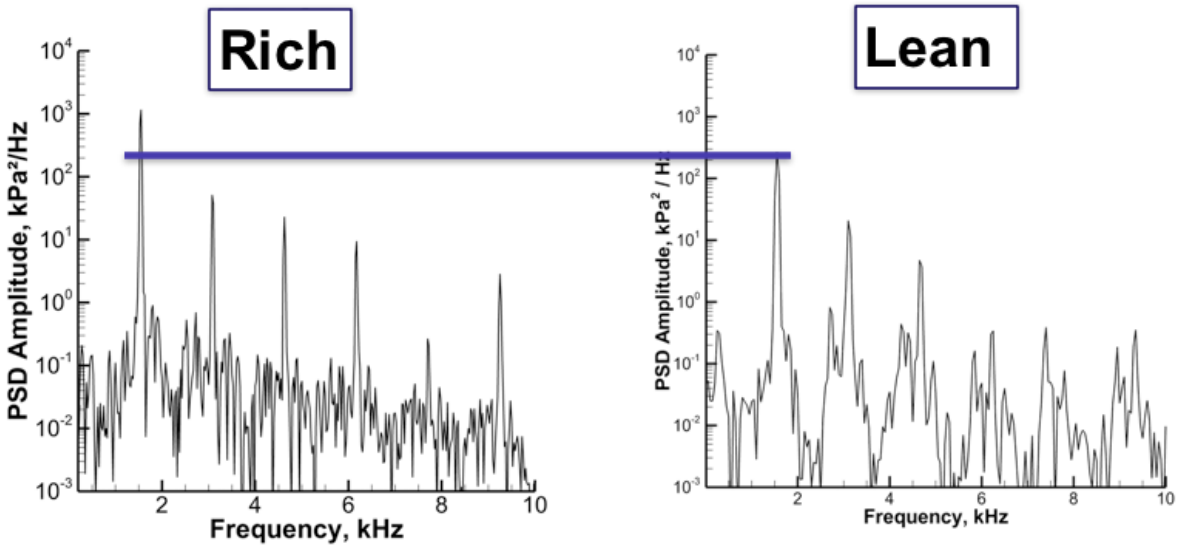

Figure 10: Comparison of the predicted PSD's for the fuel-rich and fuel-lean cases [12].

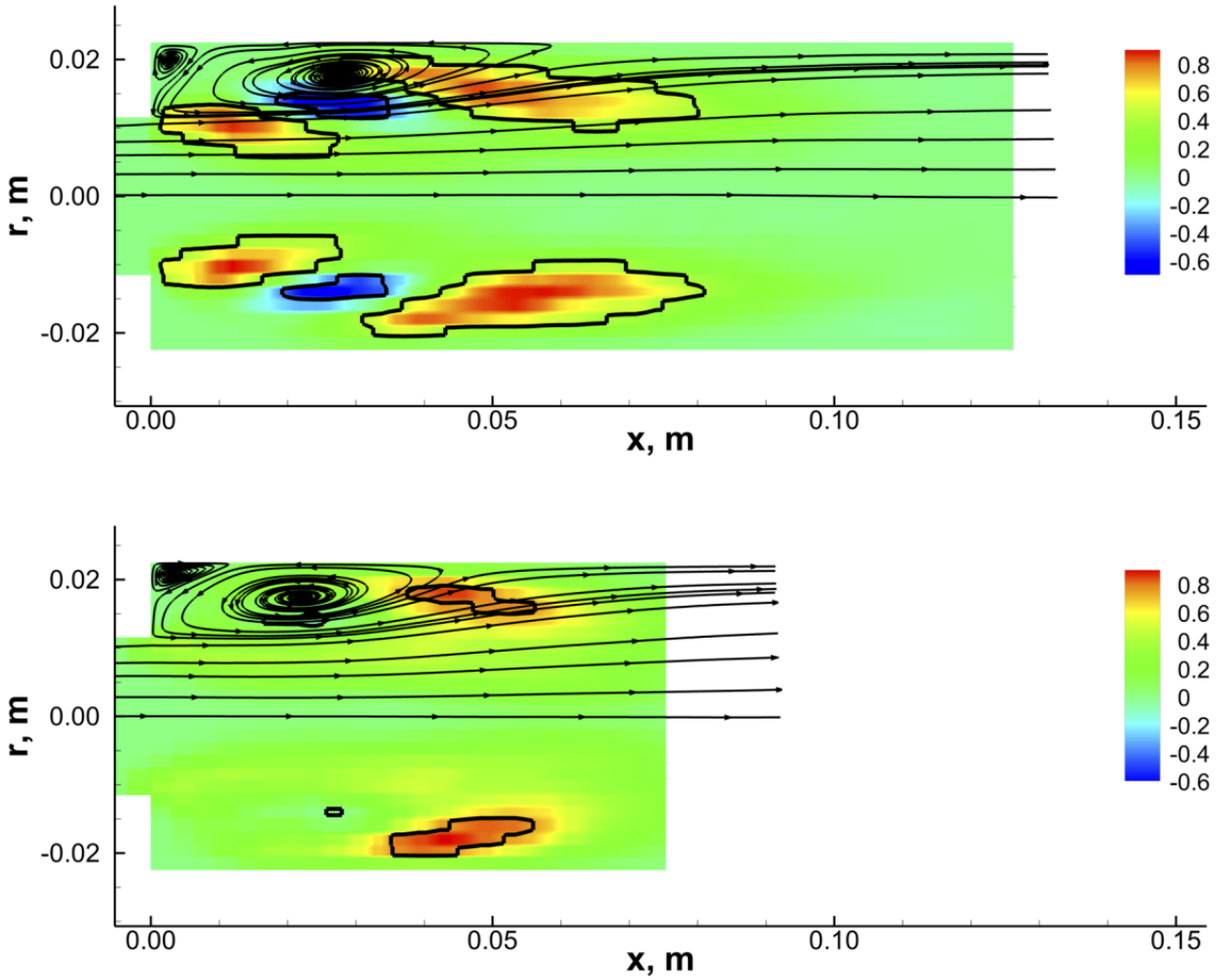

Figure 11: Contours of the computed Rayleigh index for the fuel-lean (top) and fuel-rich (bottom) cases [12].

by the axisymmetric cases. Comparisons of the vorticity in the oxidizer post indicate that vorticity that is generated downstream of the choked slot inlet are not properly damped by the axisymmetric simulations due to the lack of the vortex stretching term and may be one of the main causes of the lack of quantitative agreement.

Results of the mode-shapes in the oxidizer post and the combustion chamber indicate that the tuning of the oxidizer post results in significant changes in the resonant frequencies of the CVRC configuration, which are in turn responsible for the coupling and excitation of the instability modes. In particular, we note that the inlet boundary conditions of the oxidizer post are enforced at the oxidizer manifold, which is acoustically isolated from the combustion chamber. This appears to be of significance in properly predicting the mode shapes and therefore the combustion response. Finally, the computational data is post-processed to calculate the Rayleigh index, which shows significant regions of positive correlation between the pressure and the heat release, confirming the presence of combustion instability as the driving mechanism. Moreover, the Rayleigh index for the fuel-rich case indicates the presence of only positive coupling regions, while that for the fuel-lean case show both positive and negative coupling regions. This result is consistent with the observation that the fuel-rich case is more unstable than the fuel-lean case and provides an important diagnostic for deriving combustion response mechanisms for different experimental configurations.

Future work will focus on transverse acoustic modes, different injector elements, fuel-oxidizer combinations, multiple injectors, higher pressures, etc. The importance of including more detailed chemical kinetics and turbulent combustion closure models for combustion instability prediction will also be addressed.

References

[1] J.C. Oefelein and V. Yang. Comprehensive review of liquid-propellant combustion instabilities in f-1 engines. *Journal of Propulsion and Power*, 9(5):657–677, September-October 1993.

[2] F.S. Blomshield. Historical perspective of combustion instability in motors: Case studies. In *37th AIAA/ASME/SAE/ASEE Joint Propulsion Conference and Exhibit*, Salt Lake City, Utah, July 2001.

[3] F.E.C. Culick. Combustion instabilities: Mating dance of chemical, combustion, and combustor dynamics. In *36th Annual AIAA/ASME/SAE/ASEE Joint Propulsion Conference and Exhibit*, Huntsville Alabama, July 2000.

[4] D.T. Harrje and F.H. Reardon. Liquid propellant rocket combustion instability. Technical Report SP-194, NASA, Washington D.C., 1972.

[5] S. Ducruix, T. Schuller, D. Durox, and S. Candel. Combustion dynamics and instabilities: Elementary coupling and driving mechanisms. *Journal of Propulsion and Power*, 19(5):722–734, 2003.

[6] J.W.S. Rayleigh. The explanation of certain acoustical phenomena. *Nature*, 18:319–321, 1878.

[7] F.E.C. Culick, M.V. Heitor, and J.H. Whitelaw, editors. *Unsteady Combustion*. NATO Science Series E. Springer, New York, 1996.

[8] Y.C. Yu. *Experimental and analytical investigations of longitudinal combustion instability in a continuously variable resonance combustor (CVRC)*. PhD dissertation, Purdue University, West Lafayette, IN, August 2009.

[9] S.C. Rosen. *Combustion instabilties in the transition region of an unstable model rocket combustor*. Masters thesis, Purdue University, West Lafayette, IN, August 2011.

[10] T.W. Feldman, M.E. Harvazinski, C.L. Merkle, and W.E. Anderson. Comparison between simulation and measurment of self-excited combuistion instability. In *48th AIAA/ASME/SAE/ASEE Joint Propulsion Conference and Exhibit*, Atlanta, GA, July 2012. AIAA.

[11] R.J. Smith. *Computational Investigations Of High Frequency Acoustics And Instabilities In a Single-Element Rocket Combustor*. Dissertation, Purdue University, West Lafayette, August 2010.

[12] M.E. Harvazinski. *Modeling Self-Excited Combustion Instabilities Using a Combination of Two- and Three-Dimensional Simulations*. Dissertation, Purdue University, West Lafayette, May 2012.

[13] D.C. Wilcox. *Turbulence modeling for CFD*. DCW Industries, La Canada, CA, 1998.

[14] D.C. Wilcox. Formulation of the k-ω turbulence model revisited. In *45th AIAA Aerospace Sciences Meeting and Exhibit*, Reno, NV, January 2007. AIAA.

[15] P.R. Spalart, W.H. Jou, M. Strelets, and S.R. Allmaras. Comments on the feasibility of LES for wings on a hybrid RANS-LES approach. In *1st U.S. Air Force Office of Scientific Research Office Conference on DNS/LES*, pages 137–148, Columbus, OH, August 1997.

[16] A. Travin, M. Shur, and P.R. Splart. Physical and numerical upgrades in the detached-eddy simulation of complex turbulent flows. In *412 EUROMECH Colloquium on LES of Complex Transitional and Turbulence Flows*, Munich, October 2000.

[17] D. Li, C.L. Merkle, and G. Xia. Analysis of real fluid flows in converging diverging nozzles. In *33rd AIAA Fluid Dynamics Conference and Exhibit*, June 2003. AIAA Paper 2003-4132.

[18] D. Li, G. Xia, V. Sankaran, and C.L. Merkle. Computational framework for complex fluids applications. In *3rd International Conference on Computational Fluid Dynamics*, Toronto, Canada, July 2004.

[19] D. Li, V Sankaran, C.L. Merkle, and J Lindau. A unified computational formulation for multi-component and multi-phase flows. In *43rd AIAA Aerospace Sciences Meeting and Exhibit*, January 2005. AIAA Paper 2005-1391.

[20] C. Lian, G. Xia, and C.L. Merkle. Solution-limited time stepping to enhance reliability in cfd applications. *Journal of Computational Physics*, 228:4836–4857, 2009.

[21] C. Lian, G. Xia, and C.L. Merkle. Impact of source terms on reliability of cfd algorithms. In *The 19th AIAA Computational Fluid Dynamics*, San Antonio, TX, June 2009.

[22] G. Xia, V. Sankaran, D. Li, and C.L. Merkle. Modeling of turbulent mixing layer dynamics in ultra-high pressure flows. In *36th AIAA Fluid Dynamics Conference and Exhibit*, San Francisco, CA, June 2006. AIAA Paper 2006-3729.

[23] G. Xia, M.E. Harvazinski, and C.L. Merkle. Investigation of modeling and physical parameters on instability prediction in a model rocket combustor. In *47th AIAA/ASME/SAE/ASEE Joint Propulsion Conference and Exhibit*, San Diego, CA, July 2011. AIAA Paper 2011-6030.

[24] M.E. Harvazinski, W.E. Anderson, and C.L. Merkle. Combustion instability diagnostics using the rayleigh index. In *47th AIAA/ASME/SAE/ASEE Joint Propulsion Conference and Exhibit*, San Diego, CA, July 2011. AIAA Paper 2011-5548.

[25] M.E. Harvazinski, G. Xia, W.E. Anderson, and C.L. Merkle. Analysis of self-excited combustion instability using a combination of two- and three-dimensional simulations. In *48th AIAA Aerospace Sciences Meeting*, Nashville, TN, January 2012. AIAA Paper 2012-782.